Published in final edited form as:
Mitochondrion. 2011 January ; 11(1): 76–82. doi:10.1016/j.mito.2010.07.007.

Upregulation of Human Selenoprotein H in murine hippocampal neuronal cells promotes mitochondrial biogenesis and functional performance

Natalia Mendelev, **Suresh L. Mehta**, **Sam Witherspoon**, **Qingping He**, **Jonathan Z. Sexton**, and **P. Andy Li***
Department of Pharmaceutical Sciences, Biomanufacturing Research Institute and Technological Enterprise (BRITE), North Carolina Central University, Durham, NC 27707, USA

Abstract

Overexpression of selenoprotein H (SelH) gene provides neuroprotection in neurons against UVB-induced cell death by blocking the mitohcondria-initiated apoptotic cell death pathway. This study examined the effects of SelH on mitochondrial biogenesis and mitochondrial function. The results demonstrated that overexpression of SelH gene in neuronal HT22 cells significantly increased the levels of mitochondrial biogenesis regulators, nuclear respiratory factor-1 (NRF-1), peroxisome proliferator-activated receptor- coactivator-1 alpha (PGC-1α) and mitochondrial transcription factor A (Tfam). Mitochondrial cytochrome *c* content was elevated, mass was increased and respiration was enhanced. SelH transfection ameliorated ultra violet B (UVB)-induced suppression of mitochondrial biogenesis markers and depolarization of mitochondrial membrane potential. Overexpression of SelH promotes mitochondrial biogenesis and improves mitochondrial functional performance.

Keywords

Mitochondrion; Mitochondrial biogenesis; Mitochondrial respiration; Neuron; Selenoprotein; cell signaling

1. Introduction

Among the 25 selenoproteins identified to date, some of them are well known for their anti-oxidant properties such as glutathione peroxidases (GPXs), phospholipid hydroperoxide glutathione peroxidases (PHGPXs) and thioredoxin reductases (TRs), while other still need to be characterized functionally. Selenoprotein H (SelH) has emerged as an important member in this family. Studies have shown that down-regulation of *SelH* increases the sensitivity of mouse lung cancer LCC1 cells to hydrogen peroxide challenge (Novoselov et al., 2007) and decreases cell viability and antioxidant concentrations in Drosophila

*Correspondence author: P. Andy Li, Department of Pharmaceutical Sciences, North Carolina Central University, BRITE Building 2025, 302 East Lawson Street, Durham, NC 27707, Fax: 919-530-6600, pli@nccu.edu.

Conflict of interest
The authors declare that there are no conflicts of interest

(Morozova et al., 2003). In contrast, upregulation of SelH results in increased levels of glutathione, total antioxidant capacities, and glutathione peroxidase enzyme activity in murine hippocampal neuronal HT22 cells treated with glutathione depleting agent l-buthionine(S, R)-sulfoximine (Panee et al., 2007). Studies using HT22 cells transfected with the human SelH gene have revealed that overexpression of SelH reduces accumulation of superoxide in the cells and protects cells against ultra violet B (UVB) irradiation induced damage (Ben Jilani et al., 2007). Further studies demonstrated that SelH may provide a neuro-protective effect against UVB induced damage by blocking the mitochondria-initiated cell death pathway, preserving mitochondrial function, and enhancing cell survival signals (Mendelev et al., 2009). Interestingly, nuclear respiratory factor-1 (NRF-1) protein levels are elevated in SelH-transfected (SelH-HT22) cells without or with UVB-treatment compared to vector-transfected HT22 (vector-HT22) cells. Since NRF-1 plays an important role in regulating mitochondrial biogenesis, we hypothesize that overexpression of SelH promotes mitochondrial biogenesis, thereby enhancing mitochondrial functional performance. The objective of this study was to examine the protein profiles that are related to mitochondrial biogenesis in the SelH-HT22 and vector-HT22 cells. To reach this goal, we performed 2 sets of experiments. First, we tested whether transfection of the human SelH gene promotes mitochondrial biogenesis regulating factors in non-UVB treated SelH- and vector-HT22 cells. We detected protein levels of NRF-1, peroxisome proliferator-activated receptor-γ coactivator (PGC)-1α and -1β (PGC-1α and PGC-1β), mitochondrial transcription factor A (Tfam, aka mtTFA), and cytochrome *c* using Western blot analyses; determined mitochondrial mass by using MitoTracker Green coupled with cell imaging; and measured mitochondrial respiration and oxygen consumption using oxygraph. Second, we tested whether UVB irradiation influences mitochondrial biogenesis and whether overexpression of SelH is capable of blocking the changes induced by UVB treatment. We irradiated both vector and SelH-HT22 cells with 7J/cm^2 UVB and measured the aforementioned mitochondria-related markers. Our data showed that overexpression of SelH elevated levels of mitochondrial biogenesis regulating factors, increased mitochondrial mass, and enhanced mitochondrial respiration. UVB treatment significantly suppressed mitochondrial biogenesis regulation factors and mitochondrial respiration, while overexpression of SelH was able to blunt the effects of UVB on the mitochondria.

2. Materials and methods

2.1. Cell Maintenance and Treatment

We used stably transfected murine hippocampal HT22 neuronal cells which carried either the MSCV expression vector alone or encoded hSelH. The transfection procedures and efficacy of transfection have been previously reported and showed 34-fold increase in gene levels compared to the levels of endogenous mSelH (Ben Jilani et al., 2007, Panee et al., 2007). Cells were propagated in Dulbecco's Modified Eagle Medium (DMEM)/F12 containing 10% fetal bovine serum (FBS), 2 mM glutamine, and 200 mM streptomycin/penicillin (Invitrogen) and then maintained at 90%–95% relative humidity in 5% CO_2 at 37°C. The culture medium was renewed every 3 days. All experiments were performed in triplicate with at least 2 repetitions.

2.2. UVB Irradiation

Cells were seeded in 10 cm plates and cultured to 80% cell confluence. Prior to UVB irradiation, the cultures were washed twice with cold PBS to remove residual serum and non-attached cells. Cells were incubated in serum-free medium for 1 hr and exposed to 7J/cm^2 dose of UVB radiation from a Fisher UV Transilluminator FB-TI-88A over a period of 5 min. After UVB radiation, cells were returned to the culture incubator for various periods of recovery at 37°C.

2.3. Western Blot Analysis

At 17 hrs following UVB treatment, cells were collected and lysed on ice in lysis buffer containing 20 mM Tris pH7.4, 10 mM KCL, 3 mM $MgCl_2$, 0.5% NP40 and protease inhibitor cocktail (Roche). Lysates were centrifuged at 500 *g* for 10 min and resulted in a supernatant (S1) and pellet (P1). The P1 pellet was washed twice with lysis buffer, resuspended in lysate buffer containing 1%SDS and sonicated briefly on ice (Misonix, Ultrasonic Cell Disrupter). It was then centrifuged at 20,800 *g* for 30 min. The supernatants were designated as nuclear fractions. The S1 was centrifuged at 20,000g for 20 min. The resulting supernatant was used as cytosolic fraction. The resulting pellet that contains the crude mitochondria was suspended in lysate buffer containing 1% SDS, sonicated, and centrifuged at 20,800 *g* for 30 min. the supernatant was used as mitochondrial fraction. Protein lysates were separated in 4%–12% NuPAGE BT gels (Invitrogen), transferred to PVDF membrane (Millipore) and probed with the following antibodies: NRF-1 (Santa Cruz, 1:300 dilution), PGC-1α (Cell Signaling; 1:1000 dilution), PGC-1β (Santa Cruz; 1:400), Tfam (Santa Cruz; 1:400), cytochrome *c* (Chemicon: 1:1000 dilution); and NF-κB (Sigma; 1:1000).

2.4. Mitochondrial mass detection

Ten thousands cells/well of vector and Selenoprotein H transfected cells were plated (10000 cells/well) in BioCoat Collagen1 Black/Clear 96 well plates (BD Biosciences). Cells were treated with 7J/cm^2 of UVB (as above) and were left to recover for 5h in a CO_2 incubator. Cell culture medium was substituted with serum free media containing 300 nM MitoTracker Green FM (Invitrogen); 100 μM CellTracker Red CMTPX (Invitrogen); 5 μg/ml of Hoecht33342 (Acros Organic) and incubated in the dark in a CO_2 incubator for 1 hr. After the staining incubation period, cells were washed with PBS and were returned to regular cell culture media.

A multiplexed set of three images were collected in 96-well format with the BD Pathway live-cell bioimaging system (BD Biosciences, San Jose CA) at 37°C using a 20X/0.7 NA Olympus UPlanSApo objective lens and the following excitation and emission filters for MitoTracker Green (488/10, 515LP) labeling mitochondrial mass, CellTracker Red (560/55, 645/75) to delineate the cytoplasmic boundary and Hoechst (380/10, 435LP) to identify nuclei.

Image processing was performed to quantify the total mitochondrial mass per cell using the BD Attovision software. In brief, a 100 pixel rolling-ball background subtraction was performed to correct for inhomogeneous illumination, followed by cell detection using the Hoechst/nuclear channel, cell segmentation (identification of the cytoplasmic boundary for each cell) using the CellTracker Red channel, and spot-counting and integration of the total fluorescence intensity in the MitoTracker channel. The mitochondrial mass was tabulated for each cell and then a well-level result was calculated by averaging the mitochondrial mass for each cell in a particular well.

2.5. Mitochondrial Membrane Potential Assay

Cells were grown in 10 cm plates to 70% confluence, washed with PBS twice and incubated in serum-free medium for 1 hr prior to treatment. The cells were then challenged with 7J/cm^2 of UVB and allowed to recover for 5 hrs prior to assessment of mitochondrial membrane potential. The relative mitochondrial membrane potential states of control and irradiated samples were examined via flow cytometry using the dye JC-1. Test samples were loaded (30 min at 37°C) with 2.5 μg/ml of JC-1 (Molecular Probes) and data were collected on a BD FACSAria™ cytometer using FACSDiva™ software version 6.1. Controls included “untreated” vector-HT22 and SelH-HT22 cells as well as 20 μM of carbonylcyanide p-

trifluoromethoxyphenylhydrazone (FCCP, Sigma)- treated samples providing "depolarized" populations of the two cell types. FCCP treated cells were used to produce gates separating cells exhibiting mitochondrial depolarization from those with normally polarized mitochondria. To enhance spectral separation, the red "J-aggregate" fluorescence of normally polarized mitochondria was monitored via a 610nm bandpass filter and the green fluorescence of JC-1 monomer was detected using a 530nm bandpass filter. FCCP (Molecular Probes) at 20 μM was applied to non-irradiated samples for 1 hr to generate fully depolarized controls. The resulting data files were analyzed using FlowJo™ software (Tree Star, Inc. Ashland, OR). Nested gates of forward versus side scatter and the predominate forward scatter width peak were used to limit the 2-parameter display of JC-1 fluorescence at 610 and 530 nm. Fluorescence compensation (610 minus 530) was employed during data analysis to further enhance resolution of cells with decreased mitochondrial membrane potential. The resulting 2-parameter plots of JC-1 fluorescence show population compression characteristic of electronic compensation at the lower limits of detection.

2.6. Mitochondrial O_2 consumption measurement

O_2 consumption was measured using a respirometer (Oxygraph, Oroboros Instrument) equipped with a Peltier thermostat and electromagnetic stirrer. The measurement was done in a glass chamber containing 2 ml DMEM/F12 medium with10% FBS at 37°C. The medium containing 4.3×10^{6} cells was equilibrated in ambient room air with continuous stirring (750 rpm) for 10 min. The chamber was closed to start recording the oxygen consumption at 2 second intervals and recording was stopped after stabilization of the O_2 consumption. The difference in oxygen consumption between vector-HT22 and SelH-HT22 normal and after UVB exposure was calculated using DataGraph software (Oroboros Instruments) and represented as the basal respiration.

2.7. Statistical analysis

All data were presented as means ± SD. Student's *t* test was used for analyzing data in Figure 2 and ANOVA followed by Tukey's Multiple Comparison Test was used to analyze data for Figures 4, 5B and 6. A p value <0.05 was considered as significant.

3. Results

Experiment Set I

3.1. SelH stimulates mitochondrial biogenesis markers—Three different subcellular fractions, nominally nuclear, cytosolic and mitochondrial, were used for analyses. The relative purity of these fractions was verified by the presence or absence of β–actin and COX IV in these fractions as shown in Fig. 1. Antibodies against NRF-1, PGC-1α and 1β and Tfam were blotted in the nuclear fraction (Fig. 1). Overexpression of SelH in HT22 cells significantly increased the levels of NRF-1, PGC-1α, and Tfam as compared with vector-transfected cells in the nuclear fraction. However, the PGC-1β was not increased in the nuclear lysates of the SelH-HT22 cells. Cytochrome *c* and Tfam were measured in both the cytosolic and mitochondrial fractions. The results showed that while there was no increase of Tfam in both the cytosolic and mitochondrial fractions, cytochrome *c* level was markedly increased in the mitochondrial fractions in SelH-HT22 cells (Fig. 1). Thus, overexpression of SelH increased the levels of NRF-1 and PGC-1α in the nuclear fractions and cytochrome *c* content in the mitochondrial fractions.

3.2. Changes in NF-κB—NF-κB is an inducible transcription factor localized in the cytosol at a low level. Upon stimulation, such as through inflammatory cytokines, NF-κB accumulates in the nucleus and regulates transcription of nuclear genes including PGC-1α. The NF-κB protein levels were detected in three subcellular fractions using Western

blotting. In the nuclear fractions, NF-κB level was lower in SelH-HT22 than in the vector-HT22 cells. On the contrary, its level was significantly higher in the cytosolic and mitochondrial fractions in SelH-HT22 than in the vector-HT22 cells (Fig.1).

3.3. SelH increases mitochondrial mass—One of the functions of NRF-1 and PGC-1α is to increase the synthesis of mitochondrial complex protein subunits, which may lead to increases in mitochondrial mass. To explore whether enhanced levels of NRF-1 and PGC-1α are associated with an increase in mitochondrial mass, we measured the mitochondrial mass using the integrated MitoTracker Green signal per-cell. A variable number of seamless microscopic fields were captured using the BD Pathway 855 bioimager to yield a minimum of 100 cells per well to ensure adequate statistical sampling. Images were quantified using the BD Attovision software and data analysis was performed using the JMP8 software. As shown in Fig. 2, the average MitoTracker fluorescent intensity per cell was 457.9 ± 27.3 RFU in Vector-HT22 cells and increased to 507.3 ± 74.5 in SelH-HT22 cells ($p < 0.01$). Therefore, the increases of mitochondrial biogenesis regulating markers in the SelH-HT22 cells are correlated with increased mitochondrial mass.

3.4. SelH improves mitochondrial respiration—Mitochondrial respiration was measured in both vector-HT22 and SelH-HT22 cells with high resolution respirometry. As shown in Fig. 3, mitochondrial respiration reflected by O_2 flux curve was increased in SelH-HT22 as compared to vector-HT22 cells. Correspondingly, the O_2 consumption was high in SelH-HT22, which sharply reduced the O_2 concentration and increased the respiration rate. Therefore, the basal respiration rate peaked from 39.56±2.81 in vector-HT22 to 78.54±6.13 pmol/s/ml in the SelH-HT22 cells.

Experiment Set II

3.5. SelH maintains the elevated levels of mitochondrial biogenesis markers after UVB—In Experiment set I, we found that overexpression of SelH increased protein levels of NRF-1, PGC-1α, and Tfam. Next we decided to explore if transfection of SelH would be able to sustain the increased levels of these mitochondrial biogenesis regulators after UVB-irradiation. As shown in Fig. 4, UVB irradiation decreased the protein levels of PGC-1α significantly, while it had no impact on levels of NRF-1 and Tfam in vector-HT22 cells. Overexpression of SelH sustained the levels of NRF-1, PGC-1α and Tfam after UVB irradiation. As a result, the levels of these proteins were significantly higher in UVB-treated SelH-HT22 cells than in the UVB- treated vector-HT22 cells.

3.6. SelH improves mitochondrial respiration after UVB irradiation—In the first experiment we have shown that transfection of SelH increased mitochondrial functional performance at the baseline. In this part of the study we observed that overexpression of SelH prevented the fall of mitochondrial respiration after UVB-irradiation (Fig. 5A&B). Therefore, mitochondrial respiration was decreased from peak level of 39.56±2.81 to 20.33±0.33 pmol/s/ml in the vector-HT22 cells, whereas it was maintained at a higher level in SelH-HT22 cells after UVB treatment than post-UVB, and even pre-UVB, treated vector-HT22 cells, although there was a decrease from 78.54±6.13 to 48.64±1.90 pmol/s/ml in SelH-HT22 cells after UVB treatment. If the post-UVB data was normalized against the pre-UVB data, the vector-HT22 cells had a 49% decrease, while SelH-HT22 cells had a 38% decrease post-UVB as compared to the pre-UVB levels.

3.7. SelH stabilizes mitochondrial membrane potential—Mitochondrial membrane depolarization plays an important role in mediating the release of pro-apoptotic proteins such as cytochrome *c* and apoptosis-inducing factor from the mitochondria, a critical step in the initiation of apoptotic cell death pathways. To further evaluate the impact of SelH

transfection on mitochondrial functional performance after UVB challenge, we detected mitochondrial membrane potential using JC-1 fluorescent probe. The results showed that overexpression of SelH significantly reduced the population of cells with depolarized mitochondrial membrane potential at the resting level and after UVB exposure (Fig. 6). Under serum-free control conditions there were fewer mitochondrial depolarized cells in the SelH- HT22 than in the vector-HT22 cells (9.3% *vs.* 22.1%, P<0.01, Fig. 6, Left panels). At 5 hrs following 7J/cm^2 UVB exposure, the depolarized population increased to 55.9% in the vector-HT22 cells (p<0.01). In contrast, mitochondrial membrane potential was better maintained in the SelH-HT22 cells with only 18.5% of these cells being scored as depolarized (p< 0.01 compared to UVB-treated vector-HT22 cells, Fig. 6, Middle panels). After application of 20 μM FCCP, the percentages of cells with depolarized mitochondrial membrane potential were 82.4% and 84.9% in the vector- and SelH-HT22 cells, with no significant differences noted (Fig. 6, Right panels).

4. Discussion

Our results demonstrated that transfection of human SelH gene into neuronal HT22 cells significantly increased the translational levels of NRF-1, PGC-1α and Tfam, factors regulating mitochondrial biogenesis. Both NRF-1 and PGC-1α are nuclear factors that control mitochondrial function and biogenesis. NRF-1 has been linked to the expression of nuclear genes that directly encode subunits of the five mitochondrial complexes or through binding to Tfam (Scarpulla 2002; Kelley and Scarpulla 2004). PGC-1α is capable of binding to several nuclear receptors including NRF-1, in addition to its interaction with peroxisome proliferator-activated receptors (PPAR). The binding of PGC-1α *trans*-activates NRF-1 target gene and increases mitochondrial biogenesis and oxidative function by activation of Tfam (Wu et al., 1999). It is thus proposed that upregulation of PGC-1α gene causes activations of NRF-1 and then subsequently Tfam, resulting in synthesis of mitochondrial complexes and enhanced mitochondrial functional performance. Consistent with this theory, mitochondrial cytochrome *c* content was elevated, mitochondrial mass was increased and mitochondrial respiration was enhanced in the SelH-transfected cells compared to vector-transfected cells. Our results are consistent with a previous study showing that activation of NRF-1 increases cytochrome *c* content and mitochondrial density (Bergeron et al., 2001).

The PGC-1α – NRF-1 signaling pathway could be activated by protein kinase A (PKA), and cAMP response element-binding (CREB), by calcium activated calcium/calmodulin-dependent protein kinase type IV (CaMKIV), by activation of AMPA (α-amino-3-hydroxyl-5-methyl-4-isoxazole-propionate) receptor or by cGMP (Scarpulla, 2008). It is not known through what mechanisms or which pathways SelH increases post-translation levels of mitochondrial biogenesis regulating factors. Previous studies have shown that SelH is a DNA binding protein that up-regulates genes involved in glutathione synthesis and phase II detoxification (Panee et al., 2007). It remains unknown whether SelH directly binds to nuclear factors such as NRF-1 and PGC-1α or indirectly activates other factors that controlling NRF-1 and PGC-1α.

NF-κB is a ubiquitous inducible transcription factor that controls transcription of hundreds of other genes including PGC-1α. NF-κB normally localized in the cytoplasm and translocated into the nucleus upon stimulation. Accumulation of NF-κB in the nucleus caused by tumor necrosis factor-α (TNF-α) stimulation inhibits the transcription of PGC-1α and addition of NF-κB inhibitors parthenolide or pyrrolidine dithiocarbamate increases the mRNA levels of PGC-1α (Palomer et al., 2009). Our results support these findings since a high level of PGC-1α in the nuclear fraction of the SelH-HT22 cells is associated with a low level of nuclear NF-κB. In addition to its cytosolic and nuclear location, we also detected NF-κB in the mitochondrial fraction with an increased level in the SelH-HT22 cells, which

is consistent with the report showing mitochondrial localization of NF-κB (Cogswell et al., 2003). It is not known whether NF-κB functions differently when it is localized in mitochondria as compared to nuclei.

We have previously reported that UVB irradiation induces cell death by increasing the production of superoxide, activation of caspase-9 and −3 mediated cell death pathways and increasing the levels of p53 (Ben Jilani et al., 2007; Mendelev et al., 2009). In this study we have demonstrated that UVB irradiation suppresses the levels of PGC-1α, causes mitochondrial depolarization, and impairs mitochondrial respiratory function as reflected by declined mitochondrial oxygen consumption in UVB-treated vector-HT22 cells compared with non-treated ones. These findings, together with the published data, suggest that UVB induces cell death by targeting the mitochondria, resulting in mitochondrial dysfunction. Over-expression of SelH has been shown previously to protect neuronal HT22 cells against UVB-induced damage by reducing ROS accumulation and blocking mitochondria-initiated cell death pathway (Ben Jilani et al., 2007; Mendelev et al., 2009). The present study has further demonstrated that over-expression of SelH sustains levels of NRF-1, PGC-1α and Tfam, improves mitochondrial respiration and reduces the cell population with depolarized mitochondrial membrane potential compared with UVB-treated Vector-HT22 cells.

5. Conclusion

We have demonstrated that overexpression of SelH in neuronal HT22 cells increased the levels of mitochondrial biogenesis regulators, NRF-1 and PGC-1α. Such increases were associated with increased mitochondrial protein cytochrome *c*, mitochondrial mass and mitochondrial respiration rate, suggesting SelH promotes mitochondrial biogenesis. HT22 cells transfected with human SelH sustained the levels of mitochondrial biogenesis regulators, stabilized mitochondrial membrane potential and respiration after UVB irradiation. These effects are associated with decreased levels of nuclear NF-κB.

Acknowledgments

The authors greatly appreciate the gift of the vector-HT22 and SleH-HT22 cell lines by Dr. Jun Panee for use in this study. Dr. Li's laboratory is supported by a grant from National Institute of Health (R01DK075476). The BRITE is partially funded by the Golden Leaf Foundation.

References

Ben Jilani KE, Panee J, He Q, Berry MJ, Li PA. Overexpression of selenoprotein H reduces Ht22 neuronal cell death after UVB irradiation by preventing superoxide formation. Int J Biol Sci 2007;3:198–204. [PubMed: 17389926]

Bergeron R, Ren JM, Cadman KS, Moore IK, Perret P, Pypaert M, Young LH, Semenkovich CF, Shulman GI. Chronic activation of AMP kinase results in NRF-1 activation and mitochondrial biogenesis. Am J Physiol Endocrinol Metab 2001;281:E1340–1346. [PubMed: 11701451]

Cogswell PC, Kashatus DF, Keifer JA, Guttridge DC, Reuther JY, Bristow C, Roy S, Nicholson DW, Baldwin AS Jr. NF-kappa B and I kappa B alpha are found in the mitochondria. Evidence for regulation of mitochondrial gene expression by NF-kappa B. J Biol Chem 2003;278:2963–2968. [PubMed: 12433922]

Kelly DP, Scarpulla RC. Transcriptional regulatory circuits controlling mitochondrial biogenesis and function. Genes Dev 2004;18:357–368. [PubMed: 15004004]

Mendelev N, Witherspoon S, Li PA. Overexpression of human selenoprotein H in neuronal cells ameliorates ultraviolet irradiation-induced damage by modulating cell signaling pathways. Exp Neurol 2009;220:328–334. [PubMed: 19766117]

Morozova N, Forry EP, Shahid E, Zavacki AM, Harney JW, Kraytsberg Y, Berry MJ. Antioxidant function of a novel selenoprotein in Drosophila melanogaster. Genes Cells 2003;8:963–971. [PubMed: 14750951]

Novoselov SV, Kryukov GV, Xu XM, Carlson BA, Hatfield DL, Gladyshev VN. Selenoprotein H is a nucleolar thioredoxin-like protein with a unique expression pattern. J Biol Chem 2007;282:11960–11968. [PubMed: 17337453]

Palomer X, Alvarez-Guardia D, Rodriguez-Calvo R, Coll T, Laguna JC, Davidson MM, Chan TO, Feldman AM, Vazquez-Carrera M. TNF-alpha reduces PGC-1alpha expression through NF-kappaB and p38 MAPK leading to increased glucose oxidation in a human cardiac cell model. Cardiovasc Res 2009;81:703–712. [PubMed: 19038972]

Panee J, Stoytcheva ZR, Liu W, Berry MJ. Selenoprotein H is a redox-sensing high mobility group family DNA-binding protein that up-regulates genes involved in glutathione synthesis and phase II detoxification. J Biol Chem 2007;282:23759–23765. [PubMed: 17526492]

Scarpulla RC. Transcriptional activators and coactivators in the nuclear control of mitochondrial function in mammalian cells. Gene 2002;286:81–89. [PubMed: 11943463]

Scarpulla RC. Transcriptional paradigms in mammalian mitochondrial biogenesis and function. Physiol Rev 2008;88:611–638. [PubMed: 18391175]

Wu Z, Puigserver P, Andersson U, Zhang C, Adelmant G, Mootha V, Troy A, Cinti S, Lowell B, Scarpulla RC, Spiegelman BM. Mechanisms controlling mitochondrial biogenesis and respiration through the thermogenic coactivator PGC-1. Cell 1999;98:115–124. [PubMed: 10412986]

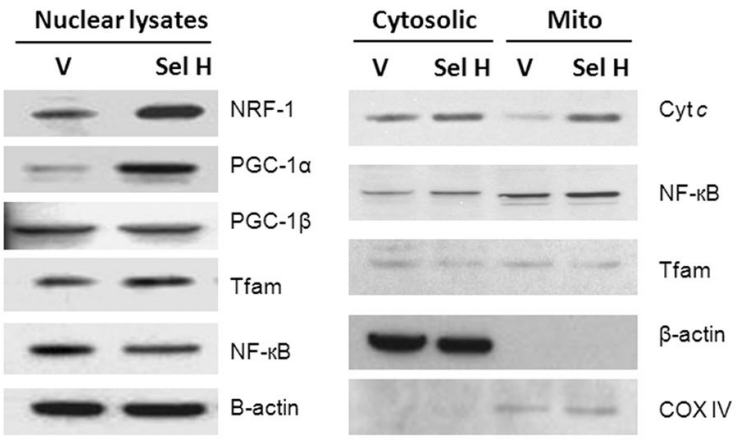

Fig. 1.

Western blot analyses of NRF-1, PGC-1α, PGC-1β, Tfam, NF-κB in the nuclear fractions and cytochrome *c* (cyt *c*), Tfam and NF-κB in the cytosolic and mitochondrial fractions of the vector-HT22 (V) and selH-HT22 (SelH) cells. Beta-actin and COX IV were loaded as internal controls. Overexpression of SelH increases the levels of NRF-1, PGC-1α and Tfam in the nuclear fraction and the levels of cytochrome c in the mitochondrial fraction. NF-κB level is decreased in the nuclear fraction and increased in the cytosolic and mitochondrial fractions in the SelH-HT22 cells.

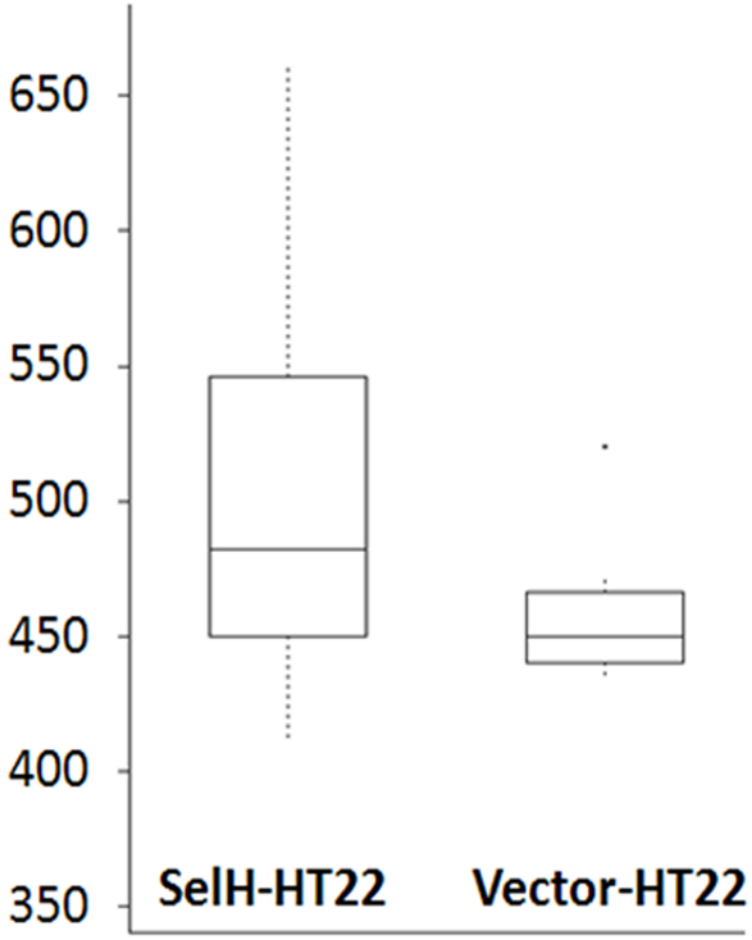

Fig. 2.

Quantification of cellular mitochondrial mass as measured by MitoTracker-Green fluorescent intensity captured on BD Pathway-855 high-content imaging system. Box-plot for SelHT22 shows significant increase in the mean (line) and quartiles (box) as compared with the control Vector-HT22. P<0.05, Student's *t* test.

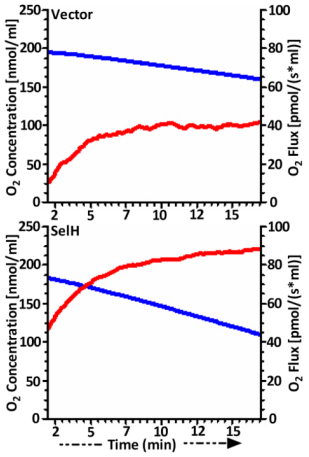

	Respiration
Vector	39.6±2.8
SelH	78.5±6.1

Fig. 3.

Mitochondrial respiration measured by oxygraph showing increased O_2 consumption and enhanced respiration in the SelH-HT22 cells. P<0.01, Student's *t* test.

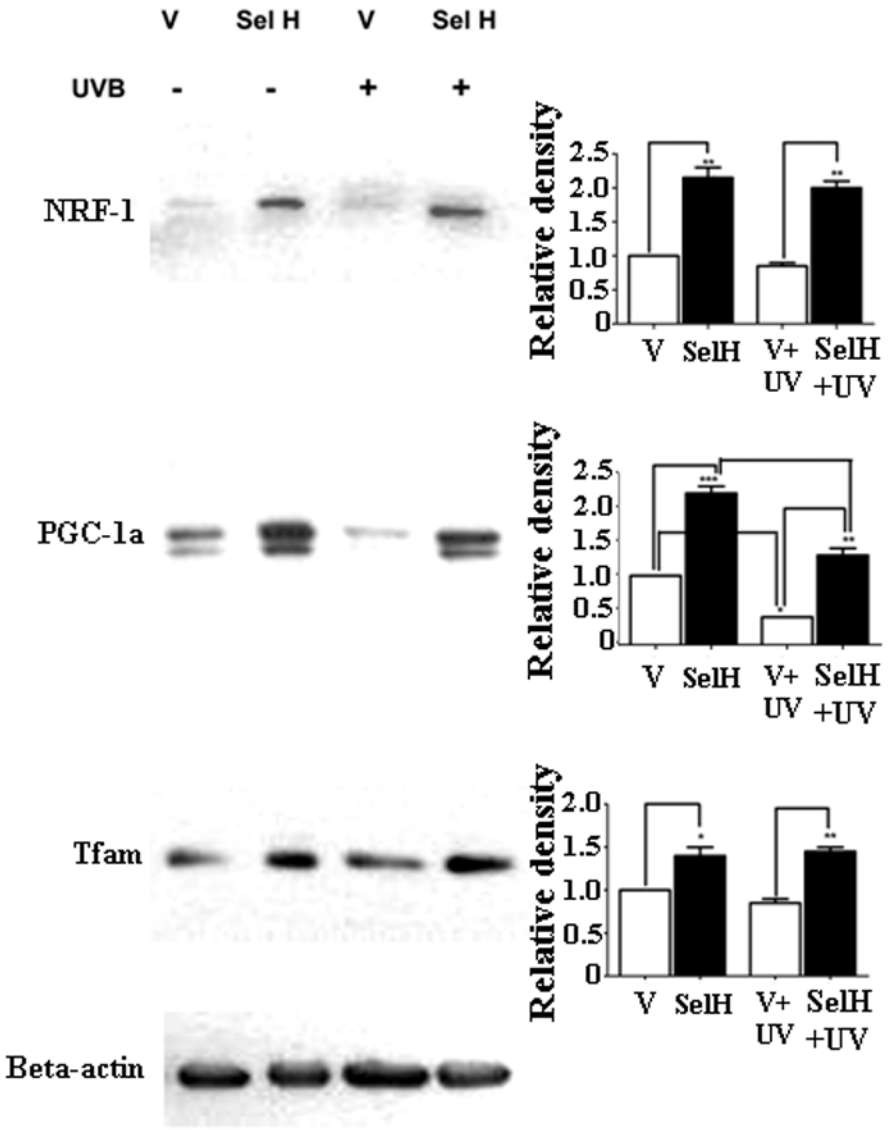

Fig. 4.

Western blot analyses of NRF-1, PGC-1α and Tfam in the nuclear fraction of vector-HT22 (V) and SelH-HT22 (SelH) cells treated with or without UVB irradiation. SelH sustains high level of NRF-1 and Tfam and prevented the fall of PGC-1α after UVB treatment. Data were collected from 2 repetitions each containing a triplicate. ANOVA analysis followed by Tukey's test. *p<0.05, ** p<0.01 and ***p<0.001, SelH *vs.* vector.

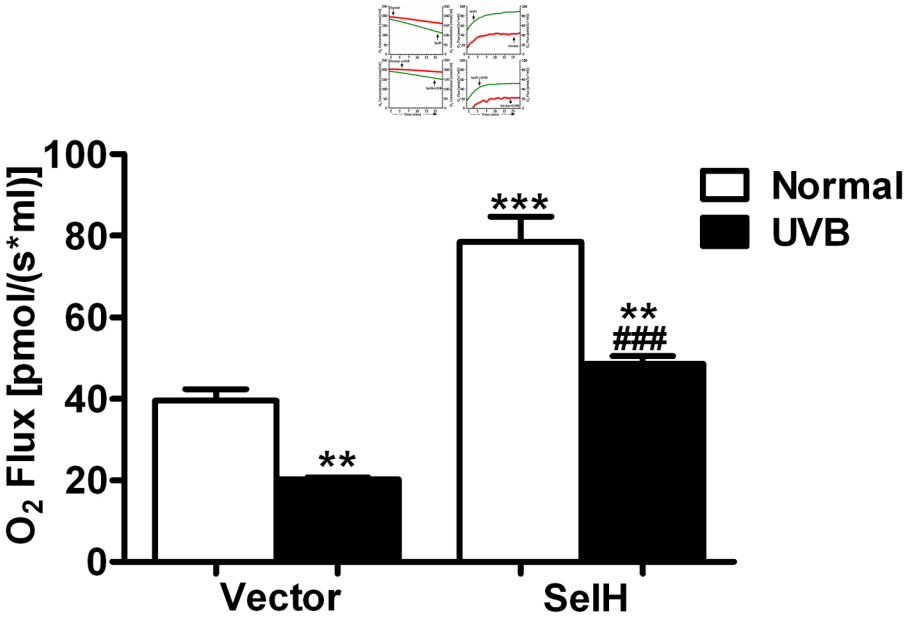

Fig. 5.

A. a representative recording showing mitochondrial oxygen consumption and respiratory rate in vector-HT22 and SelH-HT22 cells treated with or without UV irradiation. **B**. Bar graph shows the average respiratory rates in the 4 experimental groups. SelH-HT22 cells have higher respiratory rate in control status without UV irradiation. UVB treatment significantly suppressed the respiratory rate in both vector- and selH-HT22 cells, whereas the rate was significantly higher in the SelH-HT22 than the vector-HT22 cells. Data were collected from 3 independent experiments. ANOVA analysis followed by Tukey's test. ** $p<0.01$ and ***$p<0.001$ vs. non-UB treated vector-HT22 and ### $p<0.001$ vs. UV-treated vector-HT22 cells.

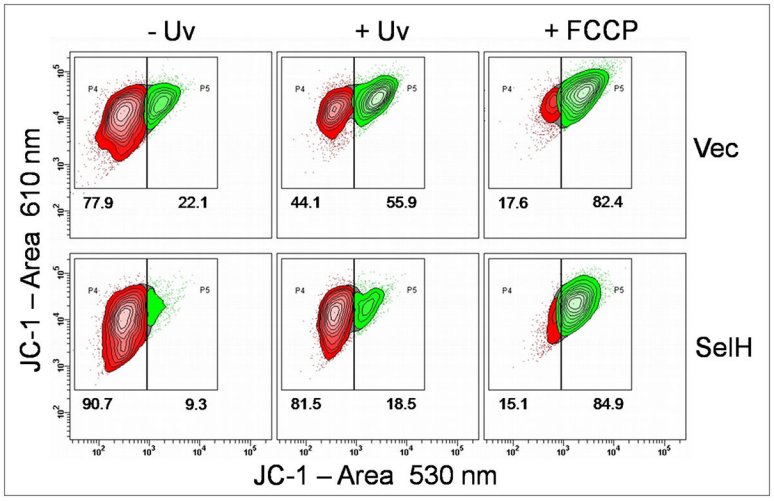

Fig. 6.

Mitochondrial membrane potential measured using JC-1 probe coupled with flow cytometry. Upper panel, vector-HT22 cells; lower panel, SelH-HT22 cells. In the absence of UVB irradiation (-UVB), SelH-HT22 cells has less cell population with depolarized mitochondrial membrane potential than the vector-HT22 cells (9.3% *vs.* 22.1%, $P<0.01$). In the presence of UVB irradiation, vector-HT22 cells with depolarized mitochondria increased significantly (55.9%), while SelH-HT22 cell had considerably less depolarized mitochondria (18.5%, $P<0.01$). After treatment of 20 μM FCCP, both SelH- and vector-HT22 cells reached more than 80% of mitochondrial depolarization (84.0% *vs.* 82.4%, $p> 0.05$). ANOVA analysis followed by Tukey's test.